Reliability-based dynamic analyses for seismic design optimization in British Columbia

Guoxi Wu, Ph.D., P.Eng.

Specialist Engineer, BC Hydro, Burnaby, BC.
& Wutec Geotechnical International, New Westminster, BC.

ABSTRACT Probabilistic based dynamic analysis of soil and concrete structures under earthquake ground motions provides an effective tool for considering uncertainties in soil parameters (Lacasse 2019) and for dealing with hazard contributions in ground motions from crustal and subduction earthquake sources. In 2017, seismic site response analyses were carried out (Wu 2017) using VERSAT-1D for a soil profile located at Roberts Bank Port (RBP) in Delta BC under 11 subduction Interface motions and 11 non-Interface (Intra-slab and Crustal) motions at various earthquake intensity levels. As a continuation of the probabilistic analyses presented in Wu (2017), recommendations for design of the 1/2,475-yr ground motions (NBCC, 2015) in the Lower Mainland are made for engineers to develop the Interface motions targeted to the 1/5,000-yr Interface spectra, develop the non-Interface motions targeted to the 1/5,000-yr non-Interface spectra, and then use in design whichever presents a higher seismic demand.

As part of a more comprehensive study, reliability method was employed to study the effect of uncertainties in soil's cyclic resistance ratio (CRR_{15}) on liquefaction potential, using discretized probability density functions for both $(N_1)_{60}$ and its correlations with CRR_{15}. On the seismic demand side, uncertainties in ground motions with 21 records and its correlation (K_M factors) with the normalized cyclic shear stress (csr_{15}) were included in the equation of reliability analysis. A total of 3465 VERSAT-1D dynamic analyses were conducted as samples (i.e., 55 samples on the Capacity side and 63 samples on the Demand side) for use in reliability analysis by sampling. The result of the reliability analysis by sampling was compared with that from the FORM approach (Foschi 2011).

The reliability method as showcased in here provides a more accurate or representative solution than the conventional factor of safety approach. The reliability analysis targets at the exact performance index, e.g., probability of liquefaction (P_{Liq}). Hopefully, the reliability method can gradually be adopted in some complex projects to optimize and improve seismic design of structures in BC, and likely reduce construction cost.

Introduction

The GSC 5th generation seismic hazard model (Atkinson and Adams 2013; Halchuk et al. 2016) used a full probability seismic hazard analysis (PSHA) to include seismic hazard from the Cascadia subduction interface earthquake (~M9). However, the Uniform Hazard Spectra (UHS) from the Geological Survey of Canada (GSC) model creates challenges to civil engineers in how to apply the UHS in engineering design. The GSC hazard model contains earthquake sources with magnitude difference in two orders (~M7 vs. ~M9); a ~M9 earthquake would have 1024 times the energy of a ~M7 earthquake.

Earthquakes from the two sources would result in order of magnitude difference in ground and structural response (such as ground displacements, soil liquefaction potential, and bending moments in bridge piers or in building columns). The large difference in structure response at a specific probability level makes it not appropriate to consolidate such response at that probability level.

As such, using the UHS from the GSC model that mixes contributions from both ~M7 and ~M9 would create dilemma in a decision.

This paper summarizes the procedure of applying the probabilistic seismic performance analysis (PSPA) for engineering analysis of structures (buildings, bridges, dams) located in southwest BC where both crustal and subduction earthquakes exist. The second part of the paper will present partial results of a more comprehensive study on reliability analysis for geotechnical problems.

1/5000-yr Spectra

The seismic hazard database for the 5th GSC model, including the 1/2475-yr spectra for the subduction interface (or Interface) and the non-Interface[1], has been extensively discussed in Wu (2017) and Wu (2018).

---

[1] Non-Interface earthquakes (~M7) are the subduction intraslab (or InSlab) and the crustal earthquakes.

Fig. 1. GSC Seismic Hazard Model Results for Roberts Bank Port (a) 1/2,475-yr spectra
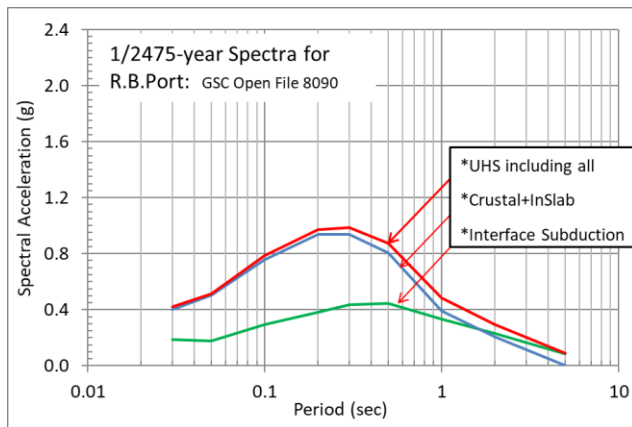
(b) 1/5,000-yr spectra
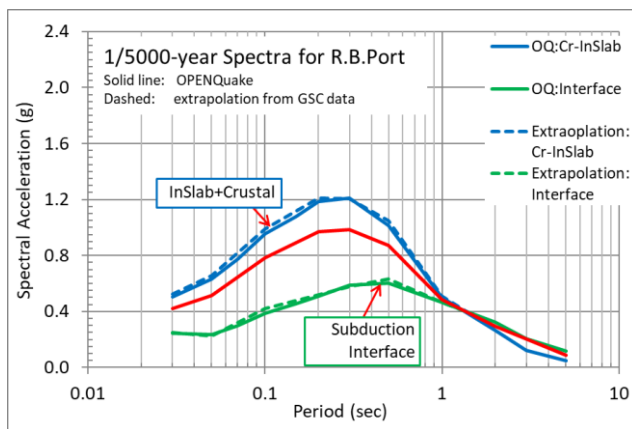
In addition to the extrapolation method described (Wu 2017), a full PSHA was conducted (Wu 2018) for three BC locations (at Vancouver, at Victoria, and at Roberts Bank Port) using the GSC model and the OpenQuake Engine (GEM 2018).

Fig. 1 shows GSC seismic hazard spectra for Roberts Bank Port at 1/2,475-yr and 1/5,000-yr levels. The 1/5000-year spectra by extrapolation (Wu 2017) are compared to the results from OpenQuake. For engineering practice, the spectra by extrapolation are well acceptable.

PSPA Approach for Seismic Slope Displacement

The PSPA method was first introduced by Wu (2017, 2018) and applied for determining the seismically induced slope displacement at a target level (e.g., 1/2475-yr) including contributions from both Interface and non-Interface earthquakes. The empirical equations developed by Bray and Travasarou (2007) were used for displacement induced by the non-Interface earthquakes (~M7); the equations by

Macedo et al. (2017) were applied for displacements by the Interface earthquakes (~M9).

Since then, Bray and Macedo (2019) have updated, based on analyses using 6711 horizontal ground motion recordings from the NGA-West2 database, the displacement equations for shallow crustal earthquakes. As such, calculations of seismic displacements are also updated; the results are shown in Fig. 2 for the Vancouver and the RBP sites.

Fig. 2. Seismic slope displacement hazard curves from empirical equations (a). A site (Ts=0.66 s, ky=0.13) in Vancouver (pt. 34044)
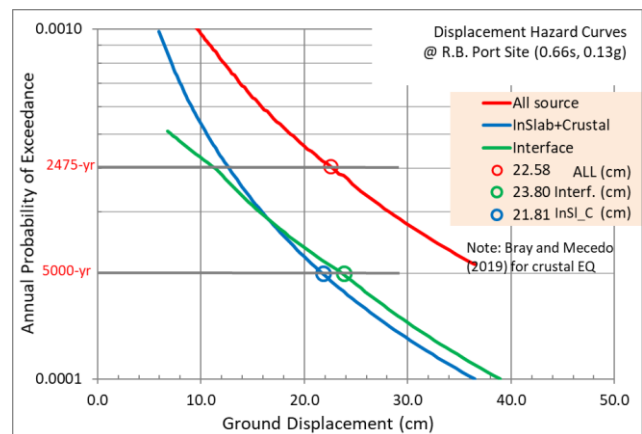
(b) Another site (Ts=0.66 s, ky=0.13) at Roberts Bank Port (pt. 34101)
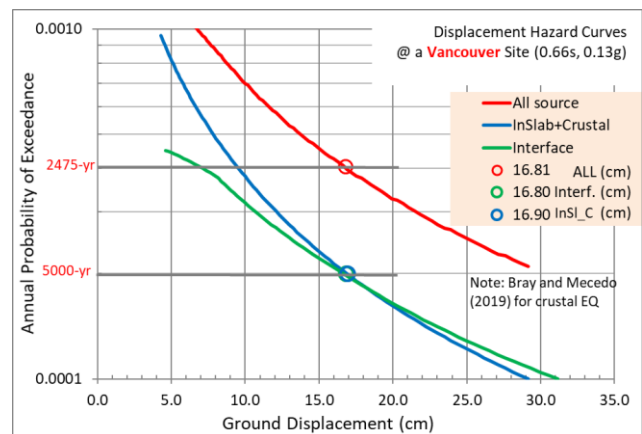
Following observations can be made from the analysis:

- Half Probability Rule: Displacements (D) from all EQ sources at 1/2475-yr level (2%/50-yr) must exist between $D_{\sim M7}$ at 1/5,000-yr level and $D_{\sim M9}$ at 1/5,000-yr level
- Largest at the Same Probability Rule: At the same probability level (1/2475-yr), D from all EQ sources is always the largest.

For the site in Vancouver at pt. 34044, the seismic displacements at 1/2475-yr from all EQ sources is

equal to $D_{\sim M7}$ at 1/5,000-yr level and also equal to $D_{\sim M9}$ at 1/5,000-yr level. Although it is purely coincidence, this demonstrates an important conclusion of this study that forms the basis of the recommendation.

PSPA Approach for Assessing Liquefaction at the 1/2475-yr Level

A borehole was drilled to about 150 m depth in 1995 at the Roberts Bank Port as a part of the study by GSC to determine the structure and geotechnical parameters of the delta and glacial stratigraphy in support of earthquake hazard studies in the region. The measured shear wave velocity (V_s) and soil stratigraphy were used to study the ground motion response of the site subject to 1/2475-yr earthquake ground motions (Wu 2017). A total of 11 input ground motion records, consisting of 6 Crustal records and 5 InSlab records, were used in the 2017 VERSAT analyses (Wu 2017).

The time histories of cyclic shear stress response for each soil element were traced by VERSAT program and used for calculation of factor of safety against liquefaction (FS_{Liq}) by cumulating equivalent number of shear stress cycles (i.e., the normalized shear stress ratio csr_{15}). In order to determine FS_{Liq} from all EQ source, the site response analyses were conducted at three levels (1/2475-yr, 1/5000-yr and 1/10,000-yr) for each of the two earthquake sources (i.e., the ~M7 or the ~M9). The PSPA method was then applied to combine the FS_{Liq} hazard curves from the two EQ sources to derive the FS_{Liq} hazard curve for the site including all source (i.e., M7+M9).

The FS_{Liq} analysis was conducted, to illustrate merits of the PSPA method, by using an assumed $(N_1)_{60} = 24$ for soils between 4 to 30 m depth. Some of the results are shown in Fig. 4. It is clear that use of individual source (~M7 or ~M9) at the 1/2475-yr level will result in very unconservative assessment (i.e., too high FS_{Liq}) on liquefaction potential (Fig. 4a). FS_{Liq} from all EQ sources (M7+M9), that are calculated using the PSPA method, falls in between FS_{Liq} for ~M9 at the 1/5,000-yr level and FS_{Liq} for ~M7 at the 1/5,000-yr level.

## Soil Reliability against Liquefaction Non-Interface at the 1/5000-yr Level

In an effort to study the reliability of sandy soils against liquefaction, uncertainties of soil liquefaction for the soil layer between 4 and 12 m depth (Layer 2 in Fig. 3b) were characterized by using discretized (rather than continuous) probability density function for the $(N_1)_{60}$ and the probability correlations between

the $(N_1)_{60}$ and CRR_{15}[2]. The discretized probability weights for $(N_1)_{60}$ and CRR_{15} that were used in the base analysis are listed in Tables 1 and 2. The cumulative probability distribution function (CDF) for crr_{15} (the Capacity) is shown in Fig. 5. The other soil parameters such as V_s, shear modulus reduction and soil damping variations with shear strains, are considered to be deterministic, i.e., not stochastic variables.

Fig. 3. GSC Seismic Hazard Curves for Roberts Bank Port (a) FD95-S1 data and V_s used in VERSAT
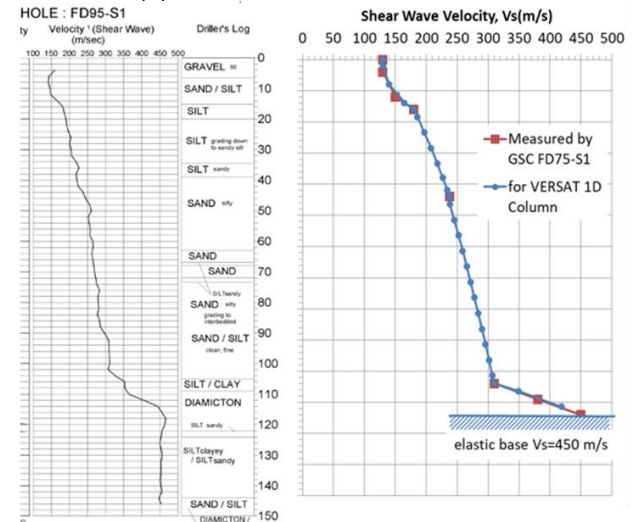
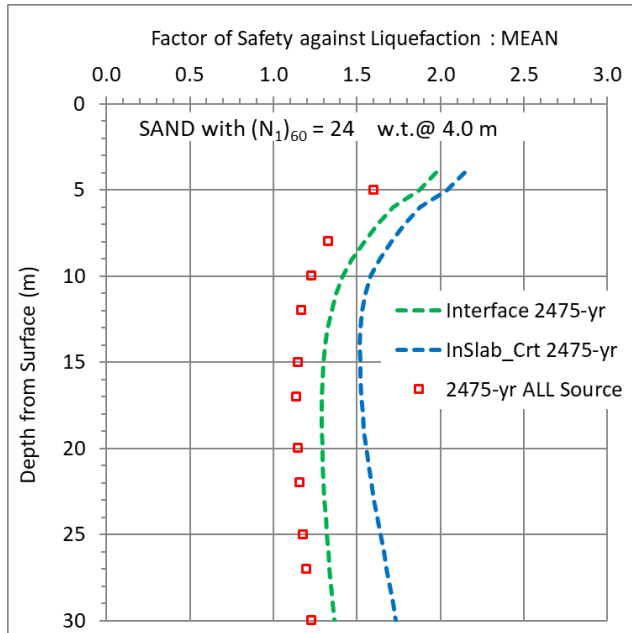(b) VERSAT model for 1D site response analyses

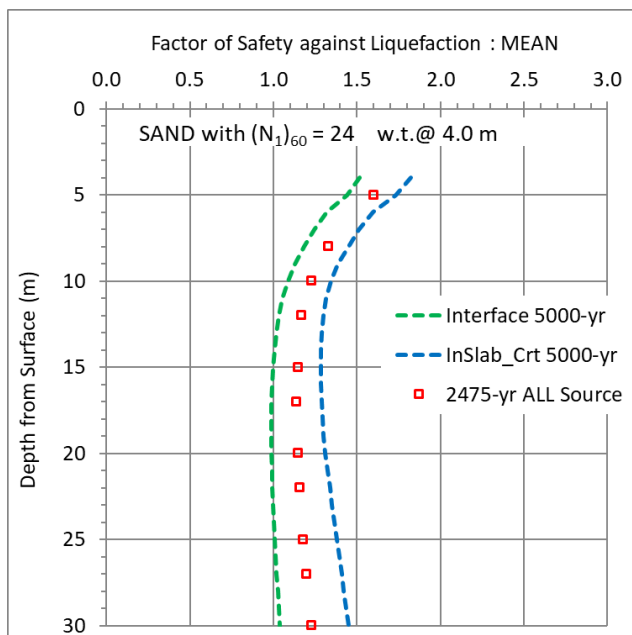

elastic base Vs=450 m/s

---
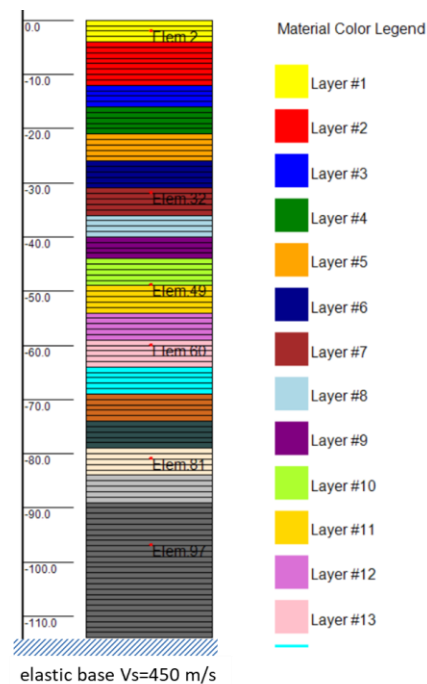
[2] The cyclic resistance ratio CRR_{15} is the ratio of cyclic shear stress (over 101.3 kPa) required to cause liquefaction in 15 cycles of soil at an overburden stress of 101.3 kPa.

Fig. 4. Factor of Safety against Liquefaction (FS$_{Liq}$) [1] for assumed $(N_1)_{60} = 24$

(a) 1/2,475-yr ground motions

(b) 1/5,000-yr ground motions

[1] The FS$_{Liq}$ for all source (M7+M9) was derived using the PSPA method. The green and blue lines are for individual sources.
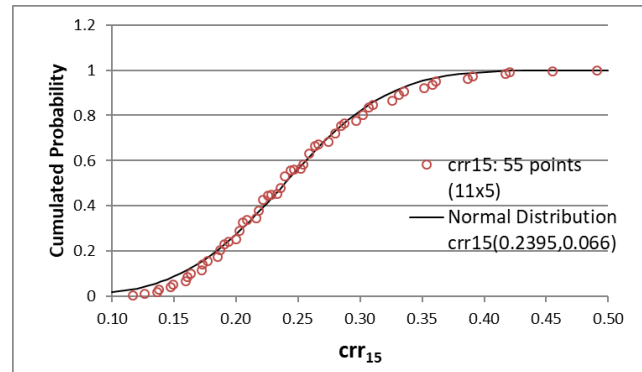
Table 1. Discretized Probability Weight: $(N_1)_{60}$ Set-A

$N_{1.60}$	19	20	21	22	23	24
Weight	0.042	0.047	0.079	0.114	0.142	0.152
$N_{1.60}$	25	26	27	28	29	$\Sigma =$
Weight	0.142	0.114	0.079	0.047	0.042	**1.0**

Table 2. Discretized Probability Weight of CRR$_{15}$

Cetin et al. (2004)	5%	20%	50%	80%	95%
Weight	0.11	0.23	0.33	0.23	0.10

Fig. 5. Cumulative Probability Distribution Function (CDF) for Capacity crr$_{15}$[3] (Element 12: 11.5 m depth)

Uncertainties of input (non-Interface) ground motions at the 1/5000-yr level are represented by using 21 earthquake (EQ) records (see Table 3) and three (3) relations for correlating or converting the number of stress cycles at irregular amplitudes to the uniform amplitude that causes liquefaction in 15 cycles. The stress normalization is represented by the α factor (Wu 2001) or by the K$_M$ factor (Idriss and Boulanger 2010). In current study, three K$_M$ factors are, namely, the Seed and Idriss (1982), Idriss (1999) and Cetin et al. (2004) relations which correspond to α of 3.6, 2.85 and 2.0 in VERSAT dynamic analysis (WGI 2020).

It is noted that 21 shear stress time histories, for Element 12 at depth 11.5 m, combined with three α factors resulted in a total 63 values of csr$_{15}$[4]. The 63 csr$_{15}$ points from VERSAT dynamic analyses are shown in Fig. 6. In general, the Cetin et al (2004) relation resulted the largest normalized seismic shear stress or force (the Demand). However, for relatively weak EQ records (No. 8 Northridge EQ at LA Dam and No. 9 San Fernando EQ at Pacoima Dam) the effect is the opposite; the Seed and Idriss (1982) relation resulted in the largest Demand. The csr$_{15}$ values for the 21 EQ records, averaged on the three α factors, are shown in Fig. 7; the comparison indicates that the Imperial Valley EQ at Cerro Prieto (CPE record) is an outlier on the high demand end. The EQ records representing the median demand would be the No. 17 record (Nisqually EQ at Gig Harbour, Fire Station #5) and the No. 2 record (Northridge EQ at Chalon Rd.).

---

[3] crr$_{15}$ is equal to the CRR$_{15}$ corrected to the in-situ effective overburden stress (σ_v')

[4] csr$_{15}$ is the cyclic stress ratio normalized (corrected) to the 15 cycles

Table 3. Earthquake Ground Motion Records Linearly Scaled to fit the 1/2475-yr Non-Interface Spectra

Note: These records are further scaled up by a factor of 1.29 for the 1/5000-yr ground motions.

	Earthquake			Recording Station	N	dt	Duration	PGA	PGV	PGD	Arias Int.	5%-95%
Set	Name	Date	Magnitude		points	[sec]	(sec)	[g]	[m/s]	[m]	[m/s]	[sec]
Crustal Ground Motions								**0.434**				
1	Manjil, Iran	6/20/1990	7.37	Abbar	2300	0.02	46.0	**0.391**	0.415	0.188	4.7	29.08
2	Northridge, CA	17-Jan-1994	6.69	CHL Chalon Rd	3107	0.01	31.1	**0.354**	0.315	0.060	1.7	9.0
3	Imperial Valley, CA	15-Oct-1979	6.5	CPE_Cerro Priet	6382	0.01	63.8	**0.364**	0.25	0.113	5.7	30.0
4	Tabas, Iran	16-Sep-1978	7.35	Dayhook	1050	0.02	21.0	**0.495**	0.343	0.228	3.4	11.34
5	Turkey, Kocaeli	17-Aug-1999	7.51	Izmit	3000	0.01	30.0	**0.342**	0.574	0.358	1.8	13.3
6	Chuetsu-oki, Japan	16-Jul-2007	6.8	K.Nishiyamacho	6000	0.01	60.0	**0.426**	0.368	0.065	2.1	11.19
7	Duzce, Turkey	12-Nov-1999	7.14	Lamont 531	4150	0.01	41.5	**0.312**	0.339	0.200	2.6	14.89
8	Northridge, CA	17-Jan-1994	6.69	LA Dam	2658	0.01	26.6	**0.317**	0.469	0.239	1.3	6.5
9	San Fernando, CA	24-May-1905	6.61	PUL Pacoima Da	4172	0.01	41.7	**0.620**	0.288	0.064	2.0	7.26
10	Loma Prieta, CA	18-Oct-1989	6.93	SJTE Santa Teres	4999	0.01	50.0	**0.479**	0.493	0.404	4.0	10.1
11	Northridge, CA	17-Jan-1994	6.69	SSU Santa Susan	5725	0.01	57.3	**0.373**	0.257	0.103	2.2	7.36
12	Iran, Tabas	16-Sep-1978	7.35	TABas	1650	0.02	33.0	**0.386**	0.447	0.174	2.4	16.5
13	Chi-Chi, Taiwan	20-Sep-1999	7.62	TCU071	5040	0.01	50.4	**0.323**	0.279	0.094	3.4	24.0
14	Chi-Chi, Taiwan	20-Sep-1999	7.62	TCU129	7798	0.01	78.0	**0.582**	0.364	0.365	3.1	27.34
15	Loma Prieta, CA	18-Oct-1989	6.93	UCSC	2501	0.01	25.0	**0.862**	0.281	0.049	7.1	8.58
16	Chuetsu-oki, Japan	16-Jul-2007	6.8	Yoitamachi Yoita	6000	0.01	60.0	**0.311**	0.337	0.077	2.3	15.79
InSlab Ground Motions								**0.430**				
17	Washington Nisqually	28-Feb-2001	6.8	Gig Harbour, Fire Station	9900	0.01	99.0	**0.348**	0.323	0.136	2.4	23.5
18	Japan MiyagiOki	16-Aug-2005	7.2	MYG013	7992	0.01	79.9	**0.575**	0.415	0.049	5.6	21.5
19	Western Washington	13-Apr-1949	6.9	Olympia_1949 Highway Lab	7532	0.01	75.3	**0.351**	0.385	0.126	3.1	19.2
20	Washington Puget Sou	29-Apr-1965	6.7	Olym1965 Highway Lab	6939	0.01	69.4	**0.519**	0.319	0.114	3.0	20.8
21	Washington, Nisqually	28-Feb-2001	6.8	Olym2001 Highway Lab	8294	0.01	82.9	**0.355**	0.296	0.065	1.9	16.5

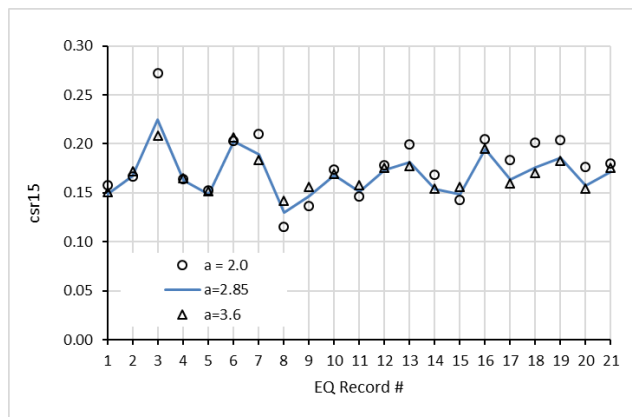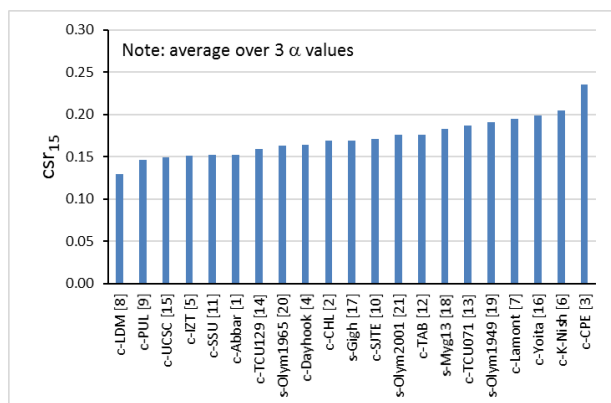**Fig. 6.** csr₁₅ from 21 EQ records and 3 α values

Fig. 7. csr₁₅ (averaged on 3 α) sorted for EQ record

Using an equal probability weight (0.0476) for each of the 21 EQ records and probability weights of 0.3, 0.4 and 0.3 for α of 3.6, 2.85 and 2.0, respectively, the cumulative probability distribution function (CDF) for csr₁₅ (the Demand) are calculated and shown in Fig. 8; the csr₁₅ points fit well with the CDF of a normal distribution with a mean (μ) or median of 0.1687 and a standard deviation (σ) of 0.02. In parallel, the Capacity crr₁₅ points in Fig. 5 fit well also with a normal distribution CDF with a median of 0.2395 and a standard deviation of 0.066.

Fig. 8. Cumulative Probability Distribution Function (CDF) for Demand csr₁₅ (Element 12: 11.5 m depth)
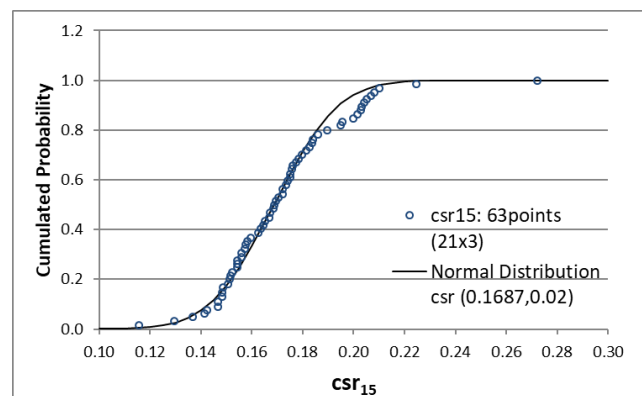
According to Foschi (2011) and Foschi et al. (2017) the performance function G for assessing soil

liquefaction would be written as (others - represent deterministic parameters):

[1] $G = crr_{15} (N_{1.60}, CRR_{15}, others) - csr_{15} (EQ \; record, \alpha, others)$

Using the first order reliability method (FORM) (Rackwitz and Fiessler 1978; Foschi 2011), the probability of liquefaction (P_f or P_{Liq}) is calculated from the reliability index (β) as $P_{Liq} = \Phi(-\beta)$, where Φ is the standard normal distribution function. Using the parameters shown in Fig. 9, the β is calculated to be 1.026 and thus $P_{Liq} = 0.152$. The reliability of soil against liquefaction is then equal to 1- $P_{Liq} = 0.848$.

A more rigorous method for reliability analysis is the so-called Monte Carlo simulation that is performed by sampling in a large amount, up to 10^6 samples in order to identify a very low probability sample. The sampling method is more suitable for a system containing irregular probability distribution functions (i.e., not normal distribution or other named distributions); it is not accurate to characterize such a system using the FORM method.

Fig. 9. Probability Density Function (PDF) for crr_{15} and csr_{15} Characterized by Normal Distributions
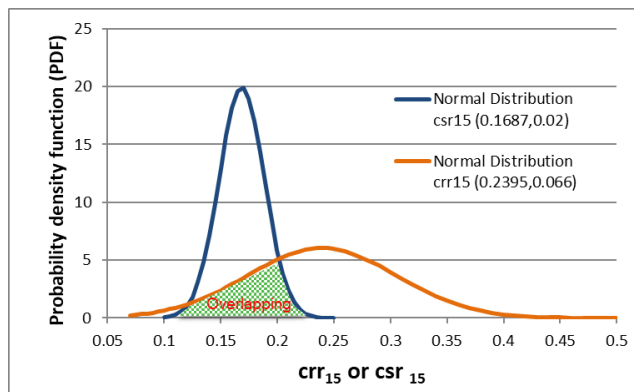
The sampling method is also adopted in the current study to examine the probability of liquefaction in order to (1) compare results with FORM; (2) apply the method to $(N_1)_{60}$ that does not have a normal distribution and (3) extend the sampling method for study of effect of earthquake induced pore water pressures on liquefaction. The sampling analysis consisted of a total of 3465 samples (i.e., 63 points of csr_{15} in Fig. 8 times 55 points of crr_{15} in Fig. 5). Instead of using the lines on the figures by FORM method, the sampling method uses the points in Fig. 5 and Fig. 8.

The CDF of FS_{Liq}[5] calculated from the sampling analysis are shown in Fig. 10. For $(N_1)_{60}$ Set-A data, assumed to have normal distribution with CDF=28%

for $(N_1)_{60} \leq 22$ (Table 1), probability of liquefaction was determined to be P_{Liq}[6] = 0.157. This compares well with $P_{Liq} = 0.152$ by FORM; it also confirms that number of samples (3465) adopted in the sampling analysis is appropriate for the study.

The $(N_1)_{60}$ Set-B data was assumed to have a biased but probably more realistic distribution with CDF=37% for $(N_1)_{60} \leq 22$ (Table 4). The CDF for Set B data are also shown in Fig. 10; P_{Liq} was determined to be 0.184 for $(N_1)_{60}$ Set-B data.

It is noted that FS_{Liq} from a deterministic analysis using $(N_1)_{60} = 24$ for Set-A and $(N_1)_{60} = 22$ for Set-B would be 1.42 and 1.20, respectively.

Table 4. Probability Weights of $(N_1)_{60}$ Set-B with CDF=37% for $(N_1)_{60} \leq 22$

$N_{1.60}$	19	20	21	22	23	24
Weight	0.04	0.06	0.12	0.15	0.15	0.14
$N_{1.60}$	25	26	27	28	29	$\Sigma =$
Weight	0.12	0.09	0.07	0.04	0.02	**1.0**

Fig. 10. Cumulative Probability Distribution Function (CDF) for FS_{Liq} (Element 12: 11.5 m depth)
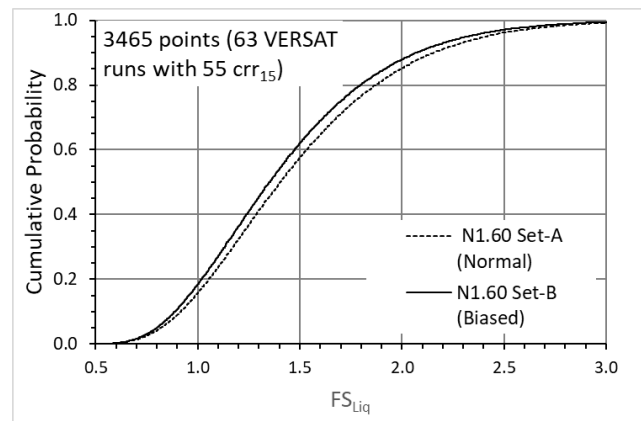
Effect of PWP on Probability of Liquefaction P_{Liq}

Effective stress analysis (Wu 2001; Finn and Wu 2013; Wu 2015; BC Hydro 2016) including the effect of seismically induced pore water pressures (PWP) on FS_{Liq} were then conducted again for the 3465 sampling points. This series of VERSAT analyses have these features:

- COV ≠ 0 because crr_{15} and csr_{15} are inter-related, coefficient of variation COV not zero.
- 3465 VERSAT-1D dynamic analyses required to generate the fragility curve for P_{Liq}.
- 3465 runs completed in 3 days in a home PC.

---

[5] FS_{Liq} in sampling analysis is the ratio of crr_{15} over csr_{15}, i.e., the same as that in VERSAT (WGI 2020).

[6] P_{Liq} is CDF for $FS_{Liq} \leq 1.0$ for sampling method; P_{Liq} is the CDF for $G \leq 0$ (i.e., $crr_{15} \leq csr_{15}$) for FORM using Eq. [1].

- P_{Liq} compiled and plotted in 30 minutes using the Automation processor built in VERSAT

It was found from the sampling analysis that effect of PWP (Fig. 11) has a major impact on P_{Liq} but little to no impact on median FS_{Liq}:

- Zero Impact on high FS_{Liq}, i.e., high $(N_1)_{60}$ portion in the fragility curve for P_{Liq}
- Little to no effect on median FS_{liq} at CDF=0.5
- Significantly reduction on P_{Liq} where FS_{Liq} ≤1.0. This is consistent with expectations that PWP has more impact where EQ shear stress is near or exceeds the liquefaction resistance,

For $(N_1)_{60}$ data with a biased distribution (Set-B), probability of liquefaction P_{Liq} increases to 0.184 from 0.157 for $(N_1)_{60}$ Set-A. However, effect of PWP reduces P_{Liq} from 0.184 to 0.130.

A summary of P_{Liq} and comparison with FS_{Liq} from deterministic analysis is presented on Table 5. Reliability based analysis with PWP indicated $P_{Liq}^{5000\_yr} = 0.130$, equivalent to an annual $P_{Liq} = 2.6 \times 10^{-5}$ for non-Interface EQ only.
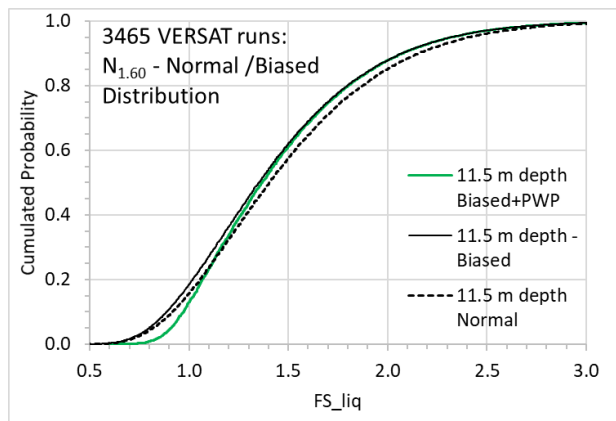
Fig. 11. Effect of PWP on CDF

Table 5. Summary Result of P_{Liq} and Comparison with FS_{Liq} from Deterministic Analysis

Analysis Method	FS_{liq}	P_{Liq}	$N_{1.60}$
Reliability Method	1.40	0.157	
above + PWP	1.42	0.108	Set-A
Deterministic: $N_{1.60}$=24	1.42	-	
Reliability Method	1.35	0.184	
above + PWP	1.37	0.130	Set-B
Deterministic: $N_{1.60}$=22	1.20	-	

Automation of 3465 Dynamic Runs by VERSAT (version 2020)

For reliability analysis of soil against liquefaction for the Roberts Bank Port soil profile, a total of 3465 dynamic runs (with PWP turned on) were completed using 11 input files, i.e., one for each $(N_1)_{60}$. While completing the 315 runs (21 non-Interface EQ records, 3 α and 5 CRR_{15}) for each $(N_1)_{60}$, the program can auto-generate hazard curves for FS_{Liq} and other response (such as ground displacement) at any pre-selected points of interest. The fragility curves in Fig. 11 were created by applying the respective weight to each $(N_1)_{60}$ and then sorting the dataset in an ascending sequence for FS_{Liq}. Once all VERSAT dynamic analyses are completed, the fragility curve in Fig. 11 can be generated and plotted in about 30 minutes. This data processing (not VERSAT dynamic runs) can be repeated for another distribution of probability weights for the 11 $(N_1)_{60}$.

Conclusion Remarks

On PSPA Approach: Use of the PSPA approach can reduce the epistemic uncertainties[7] when dealing with seismic hazard including both M9 Interface and M7 non-Interface earthquake sources.

For geotechnical analyses (such as seismic slope displacement, soil liquefaction) in the Lower Mainland, it is recommended not to use the Uniform Hazard Spectra (UHS) (such as Canada seismic hazard values from the NRC website) that mixes contributions from both the ~M7 and the ~M9 earthquake sources; not to use the 1/2475 spectra for ~M7 alone or for ~M9 alone as the design spectra for 1/2475-yr ground motions (~M7 + ~M9). Use of 1/2475 spectra from a single source (~M7 or ~M9) as the design spectra would be an error because the single source spectra are far less than the required EQ intensity; sometime, it could be only half.

It is recommended, for design in the Lower Mainland for the 1/2475-yr ground motions:

- Develop the source specific spectra, i.e., the 1/5,000-yr spectra for subduction Interface EQ (~M9) and the 1/5,000-yr spectra for non-Interface EQ (~M7). This can be done using the GSC model on the OPENQUAKE engine.
- Conduct dynamic analyses using ground motion records corresponding to the 1/5000-yr spectra.
- Do the design using the higher demand from the two sets of results (~M7 versus ~M9). If necessary, additional analyses could be conducted for refinement using 1/2475-yr or

---

7 Epistemic uncertainty (subjective uncertainty) characterizes the lack of knowledge, which is the reducible uncertainty through increased understanding (research), or increased data, or through more relevant data. It is more related to "human" or personal "belief".

1/10,000-yr spectra (for ~M7 and for ~M9) (Wu 2018)

On Reliability Analysis: Probability-based dynamic analyses (e.g., for soil liquefaction potential assessment) provide a more accurate or representative solution than the conventional factor of safety approach. The reliability analysis can account for the impact of uncertainties in soil parameters and in earthquake ground motions on the exact point of interest (P_{Liq}), not on a pseudo target (FS_{Liq}) for performance.

The efforts required for the probability-based analyses are well manageable even for engineering design. The Automation processor built in VERSAT provides the tool.

The work presented in here is the first part of a more comprehensive study aiming to develop the fragility curve for liquefaction including all earthquake sources. More works are required to characterize the probability of liquefaction for the subduction Interface EQ. In the end and hopefully, geotechnical engineers will embrace the reliability-based approach in design.

References

Atkinson, G. and Adams, J. 2013. Ground motion prediction equations for application to the 2015 national seismic hazard maps of Canada, Canadian Journal Civil Engineering 40: 988–998.

BC Hydro 2016. Seismic stability and deformation analyses of WAC Bennett Dam, BC Hydro Engineering Internal Report,

Bray, J. D., and Travasarou, T. 2007. Simplified procedure for estimating earthquake-induced deviatoric slope displacements. ASCE Journal of Geotechnical and Geoenvironmental Engineering, 1334: 381–392.

Bray, J. D., and Macedo, J. 2019. Procedure for Estimating Shear-Induced Seismic Slope Displacement for Shallow Crustal Earthquakes. ASCE Journal of Geotechnical and Geoenvironmental Engineering, 145(12)

Cetin, K. O., Seed, R. B., Der Kiureghian, A., Tokimatsu, K., Harder, L. F., Kayen, R. E., and Moss, R.E. S. 2004. Standard penetration test-based probabilistic and deterministic assessment of seismic soil liquefaction potential, J. Geotechnical and Geoenvironmental Eng., ASCE 130(12), 1314–340

Finn, W.D.L and Wu, G. 2013. Dynamic analyses of an earthfill dam on over-consolidated silt with cyclic strain softening. Keynote Lecture, 7th International Conference on Case Histories in Geotechnical Engineering, Chicago, US, April

Foschi, R.O 2011. Computational Models and Uncertainties: Estimation of Reliability and Risk. Mecánica Computacional Vol XXX, 3-21. Rosario, Argentina

Foschi, R.O., G.S. Bhuyan, R. Clark and L.M. Quiroz 2017. Hydrokinetic energy conversion systems for river applications: reliability assessment and LRFD load factors at different safety levels. Journal of Ocean Technology, Vol. 12, No. 1

Global Earthquake Model (GEM), 2018. OpenQuake Engine, https://www.globalquakemodel.org/

Halchuk, S., Adams, J., and Allen, T.I. 2016. Fifth generation seismic hazard model for Canada: crustal, in-slab, and interface hazard values for southwestern Canada. Geological Survey of Canada, Open File 8090

Idriss, I. M. 1999. An update to the Seed-Idriss simplified procedure for evaluating liquefaction potential, in Proceedings, TRB Workshop on New Approaches to Liquefaction, Publication No. FHWARD-99-165, Federal Highway Administration, January

Idriss, I. M. and Boulanger, R.W. 2010. SPT-based liquefaction triggering procedures. University of California at Davis, Report UCD/CGM-10/02

Lacasse, Suzanne. (2019) "Reliability and risk-based approaches", Keynote lecture, 2019 International Commission on Large Dams (ICOLD) Symposium on Sustainable and Safe Dams Around the World, Ottawa, June

Macedo, J., Bray, J. and Travasarou, T. 2017. Simplified procedure for estimating seismic slope displacements in subduction zones. Proceedings of the 16th World Conference on Earthquake, Santiago Chile, January

NBCC 2015. National Building Code of Canada, *by* National Research Council of Canada

Rackwitz, R. and Fiessler, B. 1978. Structural reliability under combined random load sequence. Computers and Structures, 9:5,489-494

Seed, H. B., and Idriss, I. M. 1982. Ground Motions and Soil Liquefaction During Earthquakes, Earthquake Engineering Research Institute, Oakland, CA, 134 pp

Wu, G. (2001). "Earthquake induced deformation analyses of the Upper San Fernando dam under the 1971 San Fernando earthquake". Canadian Geotechnical Journal, 38: 1-15.

Wu, G. (2015). Seismic Design of Dams, Encyclopedia of Earthquake Engineering published by Springer-Verlag Berlin Heidelberg.

Wu, G. (2017). "Probability Approach for Ground and Structure Response to GSC 2015 Seismic Hazard including Crustal and Subduction Earthquake Sources", A technical presentation on November 14, 2017 to Vancouver Geotechnical Society

Wu, G. (2018). "Probabilistic Approach to Design of Seismic Upgrade to Withstand both Crustal and Subduction Earthquake Sources", 25th Vancouver Geotechnical Society (VGS) Symposium, June

Wutec Geotechnical International (WGI, 2020). VERSAT: A Computer Program for Static and Dynamic 2-Dimensional Finite Element Analysis of Continua. Vancouver, BC, Canada